JOURNAL OF GEOPHYSICAL RESEARCH, VOL. 100, NO. C5, PAGES 8761–8776, MAY 15, 1995

The *p*H of the North Atlantic Ocean: Improvements to the global model for sound absorption in seawater

Peter G. Brewer,[1] David M. Glover, Catherine Goyet, and Deborah K. Shafer

Department of Marine Chemistry and Geochemistry, Woods Hole Oceanographic Institution
Woods Hole, Massachusetts

Abstract. At frequencies below 1 kHz, sound absorption coefficients in the ocean are a function of *p*H, and at higher frequencies they are dependent upon $MgSO_4$. The *p*H dependent terms are attributable to relaxation of $B(OH)_3$ and $MgCO_3$ species, and the ensemble effect has been approximated (Mellen et al., 1987a) as $\alpha = \alpha_1(MgSO_4) + \alpha_2(B(OH)_3) + \alpha_3(MgCO_3)$, where α is the absorption coefficient in decibels per kilometer, and $\alpha_n = (S/35)A_n[f^2 f_n/(f^2 + f_n^2)]$, where S is the salinity, A_n is the amplitude of each component and depends on *p*H, f is the frequency, and f_n is the relaxation frequency. Overall accuracy of ±15% in α requires that *p*H be known to 0.05 *p*H units. The presently used oceanic *p*H field for sound absorption models is derived from a combination of Geochemical Ocean Sections Study (GEOSECS) data and Soviet data from the 1978 Gorshkov atlas for the North Atlantic where GEOSECS data are absent. We compare the North Atlantic fields with the well-constrained Transient Tracers in the Ocean North Atlantic CO_2 data set and find large differences. We further show that sufficiently strong correlations exist between CO_2 system variables and other more commonly available hydrographic properties and that improved renditions of the *p*H field in other regions of the ocean are possible once equivalent local correlations are established, thus leading to greatly improved estimates of the sound absorption field.

1. Introduction

Accurate measurement of the oceanic CO_2 system on a global scale has long been a goal of ocean chemists and has a confusing history. Complexities in representing the *p*H scale, uncertainties in thermodynamic constants, and the need for an adequate chemical model of seawater have all contributed to the problem. The first large-scale data set was that obtained during the Geochemical Ocean Sections Study (GEOSECS) in 1972–1978; the details of the CO_2 system measurements made then are given by *Bradshaw et al.* [1981], and the data are recorded in the GEOSECS atlases.

Early work on the North Atlantic segments of GEOSECS did not produce a useful CO_2 data set owing to problems with sensor readiness, and thus a large data gap existed. This deficiency was remedied in the Transient Tracers in the Ocean (TTO) North Atlantic cruise of 1981, where, following

excellent account is to be found in the Naval Underwater Systems Center (NUSC) report by *Mellen et al.* [1987a]. Early work by *Leonard et al.* [1949] established that $MgSO_4$ was responsible for the absorption anomaly, relative to fresh waters, at frequencies in the 10- to 100-kHz range. *Eigen and Tamm* [1962] formally established the two-step equilibrium and relaxation process involved.

Schulkin and Marsh [1962] provided the first practical formula for sound absorption in seawater, and *Thorp* [1965] was able to show that an absorption anomaly, 1 order of magnitude greater than that predicted by the Schulkin and Marsh formula, existed for frequencies of about 3 kHz. The *p*H dependence of this low-frequency anomaly was subsequently confirmed by resonator experiments, and thus predictions of the low-frequency sound absorption in seawater depend upon a knowledge of the *p*H field.

Mellen et al. [1987a] have combined the chemical terms

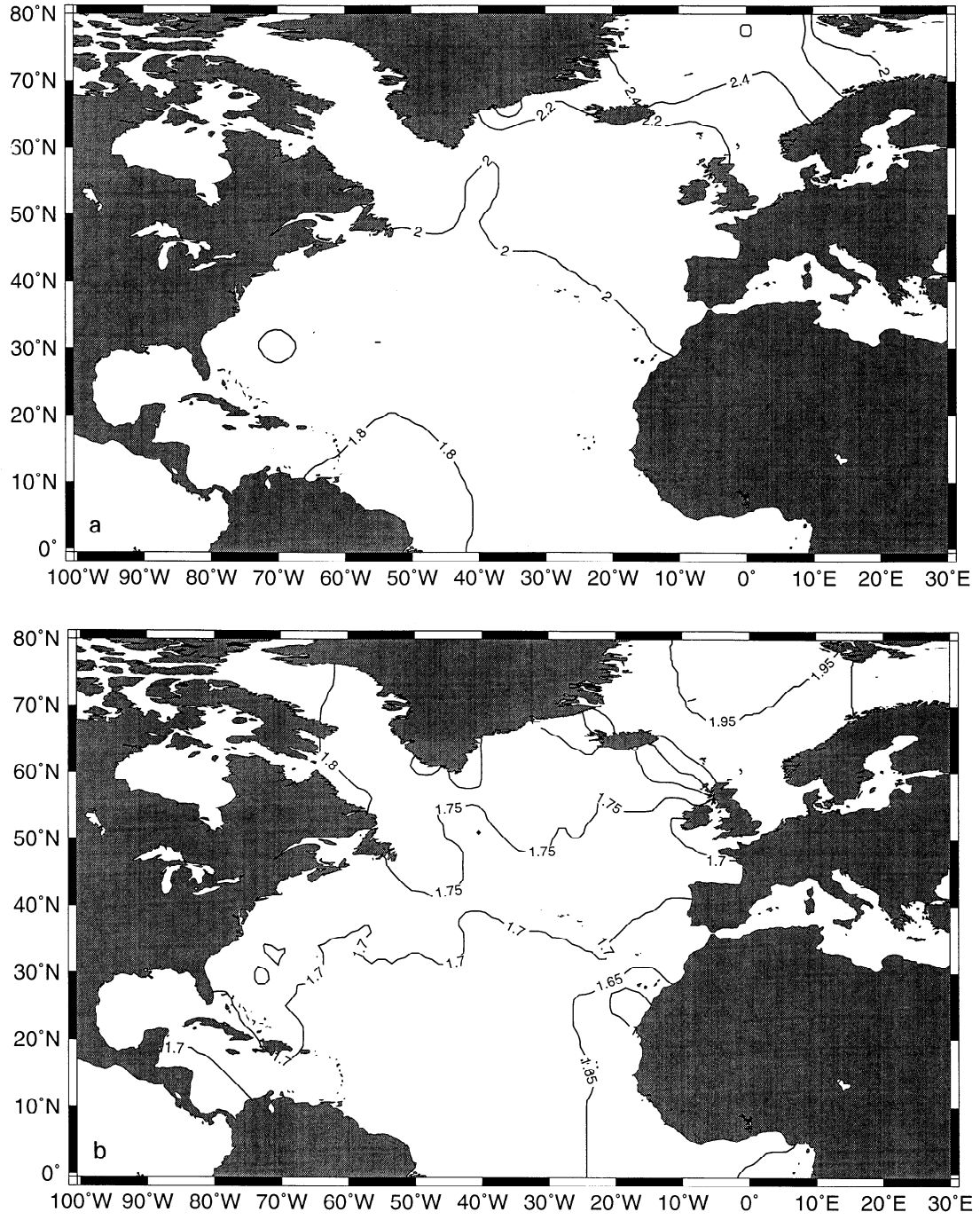

Figure 1. K_{SWS} derived from the North Atlantic Study Transient Tracers in the Ocean (TTO) data set, (a) at the surface and (b) at 2000 m. $K_{SWS} = 10^{(pH^{SWS}-7.85)}$ was used to be as compatible as possible with the K value used by *Mellen et al.* [1987a] (see Figure 2).

3. Scales for *p*H

The first problem in comparing the TTO and Gorshkov atlas data sets (Figures 1 and 2) is to establish the pH scale used. To our surprise, the pH scale is not unambiguously identified in any of the acoustic absorption literature and a brief examination of the problem is useful.

There are three pH scales in use by ocean chemists: The National Bureau of Standards (NBS, now National Institute of Standards and Technology, or NIST) pH scale (pH^{NBS}), the "free" hydrogen ion concentration scale (pm_H expressed in moles H^+ per kilogram H_2O), and the pH seawater scale (pH^{SWS} expressed in moles H^+ per kilogram solution). As clearly defined [*UNESCO*, 1987], the NBS pH scale refers to nonsaline pH buffer standards certified by the National Bureau of Standards (for example, from Sigma Chemical Co., St. Louis, Missouri). The "free" hydrogen ion concentration scale refers to fluoride-free synthetic seawater buffers Tris and Bis (Tris(hydroxymethyl)aminomethane (2-amino-2-(hydroxymethyl)-1,3-propanediol) and Bis(hydroxymethyl)methylaminomethane (2-amino-2-

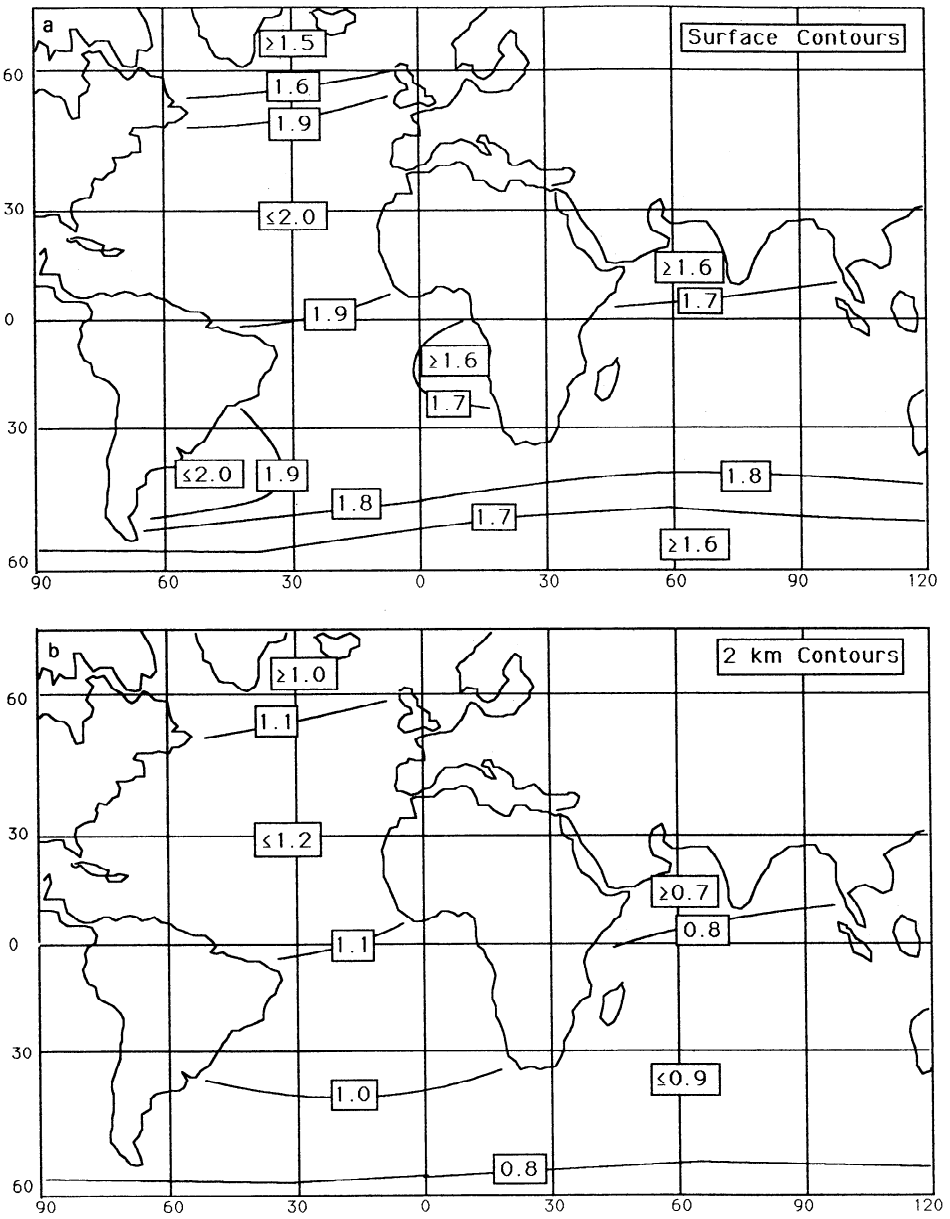

Figure 2. K (a) at the surface and (b) at 2000 m. From *Mellen et al.* [1987a, Figures 46 and 45].

methyl-1, 3-propanediol), respectively) [*Almgren et al.*, 1975; *Millero*, 1986]. The pH seawater scale refers to the total hydrogen ion concentration in the solution. The relationship between pm_H and pm_H^{SWS} (referring to $p\mathrm{H}^{SWS}$ expressed in moles H^+ per kilogram H_2O), is given by

$$pm_H^{SWS} = pm_H - \log\left[1 + \beta_{HSO_4}({}^T m_{SO_4}) + \beta_F({}^T m_F)\right] \quad (4)$$

where β_i [*Khoo et al.*, 1977] refer to the formation constants of the species HSO_4^- and HF, and where ${}^T m_X$ refer to the total analytical concentration of the SO_4^{2-} and F^- ions.

In practice, these terminology differences mean that the pH of a single seawater sample may differ by up to approximately 0.15 unit depending only upon the pH scale used. We say approximately, for there is no easy way to convert between these various scales, and an explicit thermodynamic choice must be made [*Dickson*, 1993]; however, the uncertainty in scale conversion is less than 0.01 pH unit. For measurement in seawater the $p\mathrm{H}^{SWS}$ is now recommended [*UNESCO*, 1987]; we therefore have chosen to work in this pH seawater scale (moles H^+ per kilogram solution), and the explicit values of the thermodynamic constants we use to calculate pH from measured $C_T - A_T$ pairs are reported in the appendix.

We note that since the pH value based on $p\mathrm{H}^{SWS}$ is lower than that based on $p\mathrm{H}^{NBS}$, the reference pH 8 used to determine the coefficient K should be transformed to 7.85 when referred to $p\mathrm{H}^{SWS}$. Therefore K, the pH dependent term of the sound absorption coefficient, can refer either to $K_{SWS} = 10^{(p\mathrm{H}^{SWS}-7.85)}$ or to $K_{NBS} = 10^{(p\mathrm{H}^{NBS}-8.00)}$, in other words $K \equiv K_{SWS} \equiv K_{NBS}$.

4. Data Validity

Although we suspect that equation (3), the pH contours shown in the Gorshkov atlas, and consequently the results

shown in Figure 2 were based on the pH^{NBS} scale, we will refer here only to pH^{SWS}. The reason for this is to minimize confusion, to avoid errors introduced in the passage from one pH scale to another, and to harmonize the units used by both ocean chemists and acousticians. Consequently, we express *Mellen et al.*'s [1987a] relationship giving the sound absorption coefficient as a function of pH^{SWS}:

$$\alpha_n = C_n K_{SWS} \tag{5}$$

The contours of K shown in Figure 1 are based on K_{SWS}. When *Mellen et al.* [1987a] undertook to map the coefficient K for the world ocean, they had little choice but to use the available pH data sets. Such data sets are scarce in the literature and often are presented in different formats, thus impeding an accurate compilation and comparison of the data. Where possible, they compared the pH data sets of these two sources and pointed out significant differences much larger than the desired 0.05 pH unit, which represents the minimal accuracy required for obtaining an accuracy of ±15% in the absorption coefficient α.

We believe these observed differences are due to the uncertain accuracy of the poorly described pH data set of the Gorshkov atlas. Since no details are given of the Soviet pH measurement procedure, calibration, and accuracy, it is very difficult to determine the validity of these data and to compare them with others. Furthermore, these Soviet data were displayed only as contour maps. The interval between the extrapolated contours is 0.1 pH unit, suggesting an accuracy of 0.1 pH unit for the experimental data set. As was also mentioned by *Mellen et al.* [1987a], this 0.1 pH unit spacing between contours is not accurate enough for the sound absorption model, and therefore they interpolated pH values between the contours.

The K contours, at the surface, calculated using the TTO data set (Figure 1a) are significantly higher (up to 0.9 unit) than those earlier obtained by *Mellen et al.* [1987a] using the Soviet data set (Figure 2a). A close comparison of Figures 1 and 2 reveals that K increases northward in the former and southward in the latter. Surface water chemistry is subject to significant seasonal variations. No seasonal corrections have been attempted here, and we have no information on time of year for the Gorshkov data. The TTO data were collected during the April–October period of 1981.

A comparison of the combined basin-wide depth profile of K obtained using the TTO data set (Figure 3a) with the less detailed earlier combined profiles (Figure 3b, taken from Figure 46 of *Mellen et al.* [1987b, p. 50]) further illustrates the problem. In the surface layer, K ranges from approximately 1 to 3.5 and represents approximately 4 times the variations earlier reported. We note that the higher values are observed at latitudes north of 60°N. We would expect the low pCO_2 surface waters created by photosynthesis at high latitudes in summer [*Keeling*, 1968; *Peng et al.*, 1987], and thus creating high pH and K values, would be consistent with the results reported here. Within the depth interval 500–1500 m, the minimum in K is shown strongly in Figure 3b and only weakly in the earlier GEOSECS data. Significant basin-wide variability is observed in the depth range. With the exception of results from stations located north of 60°N, Figure 3a also emphasizes the homogeneity of the coefficient K in stable water masses at depths below 2000 m.

5. Interpolation

5.1. CO_2 System Variability

For many parts of the ocean only limited coverage of CO_2 system data is available, while large and reasonably accurate data bases for hydrographic and nutrient properties exist [*Mantyla and Reid*, 1983]. We ask whether reasonable extrapolations from these properties, which may be used as ocean chemistry master variables, can be made to estimate pH in data poor regions, and we use the North Atlantic data set as a test of this hypothesis.

Strong linear correlations between geochemical variables were first recognized by *Redfield* [1942]. Geochemists identified that much of the variance of CO_2 system properties in the ocean is controlled by four functions: (1) a large stable background signal of C_T and A_T, correlated with salinity; (2) a redox dependence based upon oxidation of organic matter of approximately Redfield ratio, correlated with O_2 and the nutrients; (3) an inorganic function based upon dissolution of calcite and aragonite in surface sediments, correlated with silica; and (4) a fossil fuel invasion CO_2 term, inversely correlated with ventilation age and affecting all contemporary upper ocean waters.

In proceeding here, we have elected not to use classically defined geochemical coefficients, such as those given in the Redfield ratio, but have chosen to examine the relationship in a purely statistical manner. The overwhelming reason for this decision was to ascertain whether a small number of equations could yield statistically significant fits rather than independently specifying each geochemical function.

In order to examine these simply, we first postulate a total alkalinity relationship for the North Atlantic suggesting a relationship of the form of

$$A_T = \mathcal{F}(S,\ \theta,\ O_2,\ SiO(OH)_3^-,\ PO_4^{-3},\ NO_3^-) \tag{6}$$

We note that A_T itself is defined as a temperature independent property. *Brewer et al.* [1986] found a strong correlation between total alkalinity A_T and salinity S in the North Atlantic surface waters (Figure 4a), but as is suggested by Figure 4b, an additional term, $SiO(OH)_3^-$, is necessary to account for variance with depth.

Next we similarly examine the dependence of C_T on the same variables (Figure 5):

$$C_T = \mathcal{F}(S,\ \theta,\ O_2,\ SiO(OH)_3^-,\ PO_4^{-3},\ NO_3^-) \tag{7}$$

As a first approximation we can express these as simple linear expressions with coefficients for each term determined by a multiple linear regression. It is assumed that the fossil fuel term is folded into these correlations, and it is not explicitly separated here as a tracer related term. In fact, we expect the largest fossil fuel signal at depth to manifest itself in the North Atlantic, which should decrease the correlations. We will show that these correlations yield reliable pH values.

5.2. Correlations

5.2.1. Regressions. We have used multiple linear regression analysis to search the n-dimensional data space for the "best" fit.

Finding these relationships in multivariate space is a rather straightforward procedure. The initial procedure is to use a stepwise algorithm that finds the best subset regression of n independent variables [*Goodnight*, 1979]. We examined the combinatorics and used an algorithm that allowed us to exam-

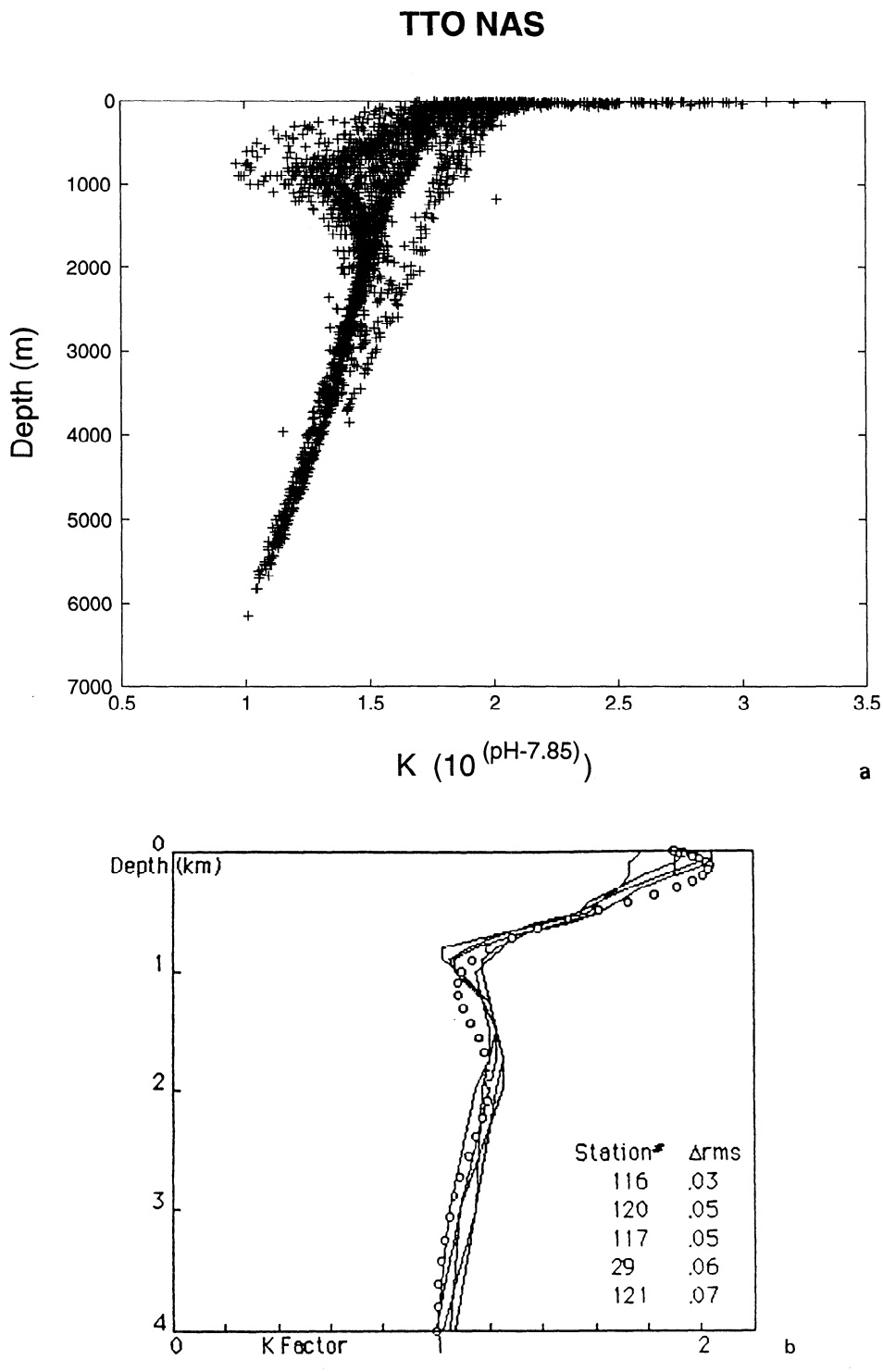

Figure 3. K versus depth. (a) K_{SWS} from TTO data. (b) K from *Mellen et al.* [1987b, Figure 46].

ine the significance of the variable order in the relationship. An algorithm based on *Efroymson* [1960] was used to do this; both of these algorithms are provided in the SAS™ mathematics package (SAS Institute, Inc., Cary, North Carolina).

The additional variability of C_T and A_T due to the seasonal variability of the mixed layer was mitigated by splitting the TTO data set into data from above and below 250 m depth. Other depth limits were also used, but this depth was found to contain virtually all of the seasonal variability in the upper layers. In this fashion, the regression analysis was divided into two components for the North Atlantic, and the additional variance due to the fossil fuel signal is, for a large part of the basin, contained within the upper regressions. However, since in high-latitude areas the seasonal variations of C_T in the surface layer is larger than the fossil fuel signal alone [*Goyet and Brewer*, 1993], the latter cannot be extracted from the available CO_2 data set.

Total alkalinity: The multiple regression of A_T against all the other measured variables in the upper 250 m of the TTO data set yields a "best" multiple linear regression by includ-

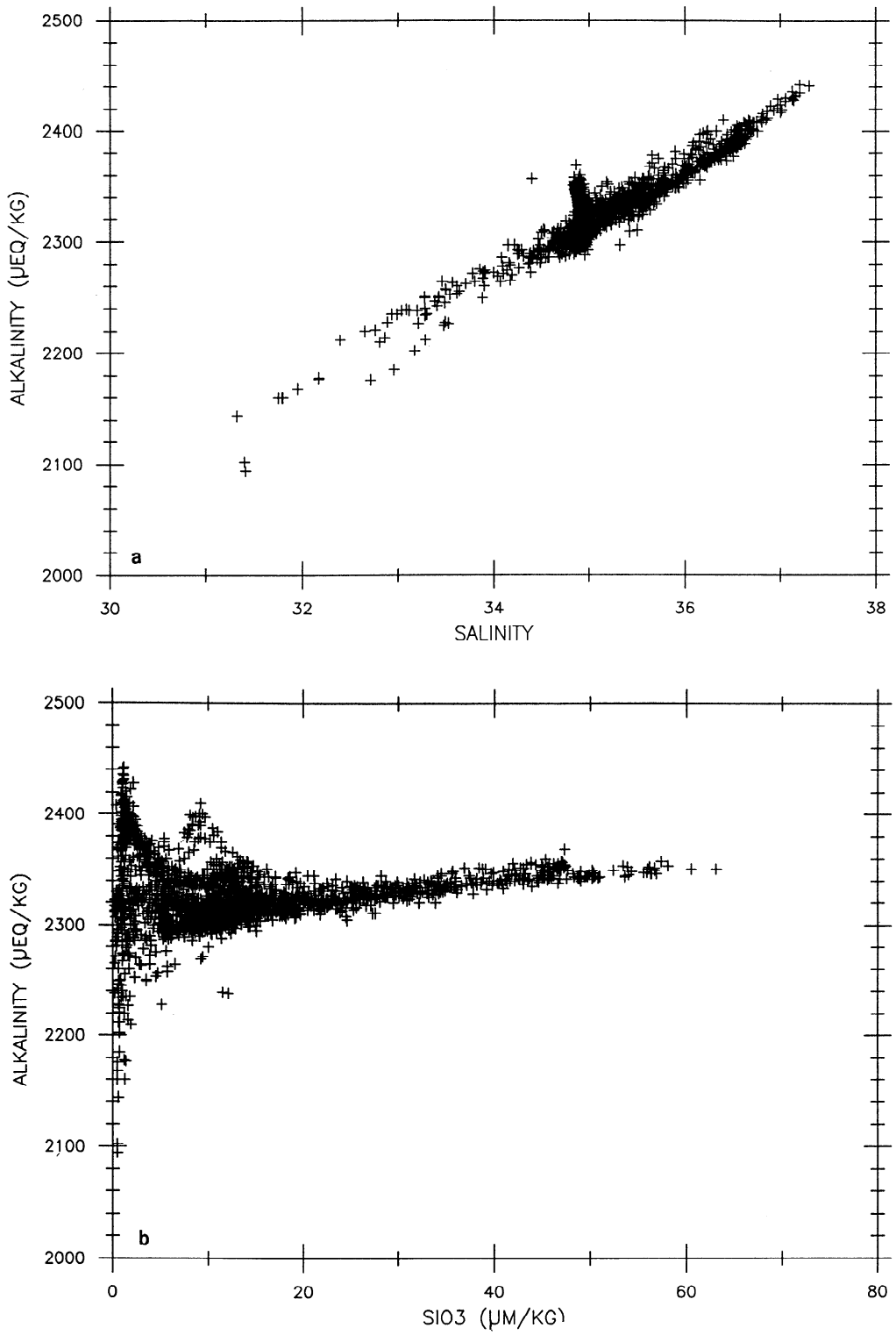

Figure 4. Scatterplots of the TTO A_T measurements versus (a) salinity and (b) $SiO(OH)_3^-$.

ing all of the possible terms except θ. Although an exceptionally high r^2 value is obtained with just S (Table 1) the C_p value [*Mallows*, 1973] does not reach an acceptable value until five of the six variables are included. The relationship is

Depth $\leq$ 250 m

$$A_T = 530 + 51.132S - 0.033O_2 + 0.973SiO(OH)_3^- + 59.3PO_4^{-3} - 4.31NO_3^- \quad (8)$$

$$r^2 = 0.975 \qquad C_p = 5.41 \qquad n = 623$$

The multiple linear regression of A_T against all the other measured variables below 250 m yielded a "best" regression employing all of the six variables (Table 1). Again this choice

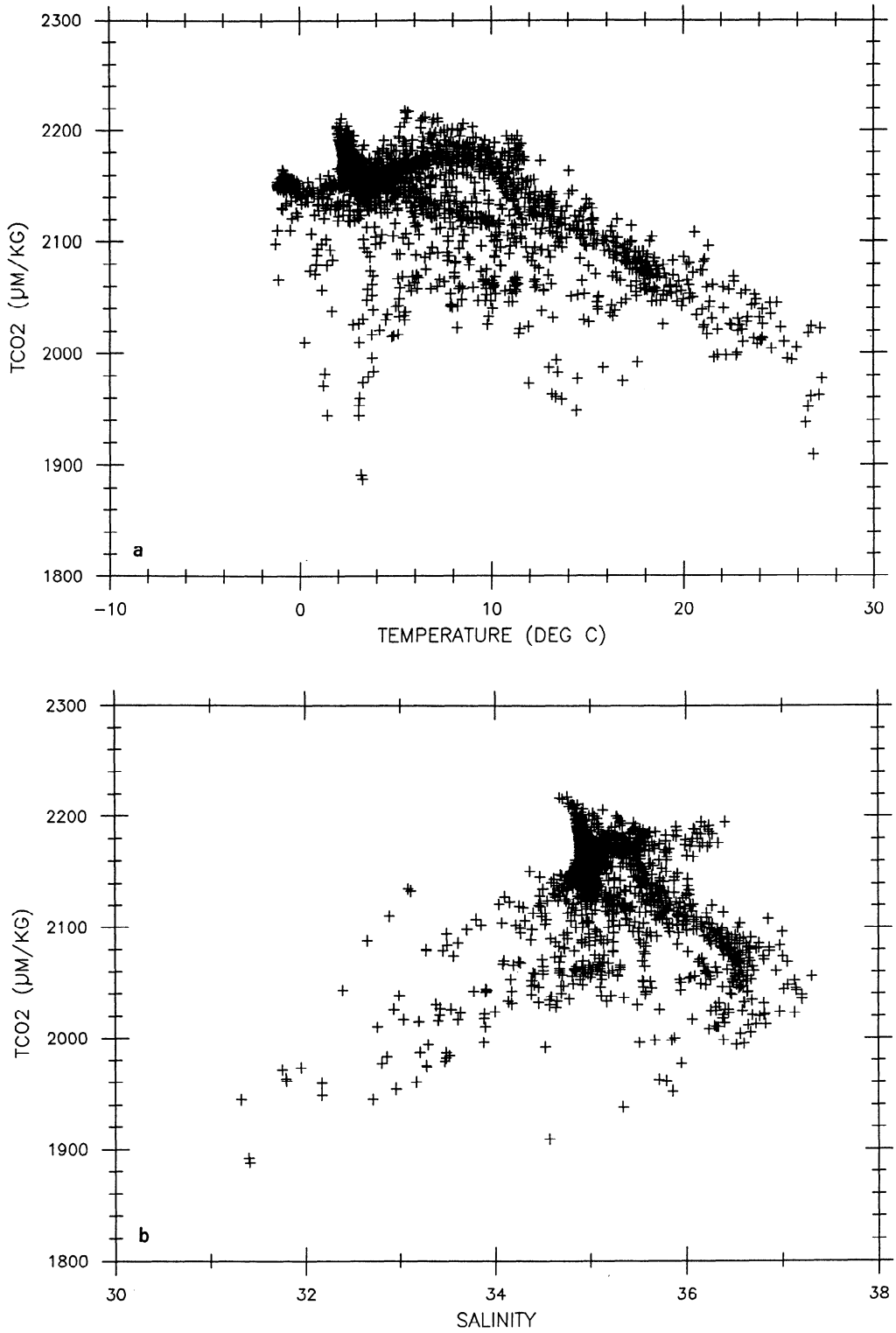

Figure 5. Scatterplots of the TTO C_T measurements versus (a) potential temperature, (b) salinity, (c) O_2, (d) PO_4^{-3}, (e) $SiO(OH)_3^-$, and (f) NO_3^-.

was guided by a slowly increasing r^2 value and a precipitously dropping C_p value. However, since C_p is a measure of the total squared error of a model with p parameters [*Mallows*, 1973] when all the variables are used, C_p will be exactly p, reflecting that this is the best that can be done with the available data set. The multiple linear regression below 250 m is

Depth > 250 m

$$A_T = -332 + 72.827S + 0.948\theta + 0.184O_2 + 0.962SiO(OH)_3^- + 44.6PO_4^{-3} - 0.970NO_3^- \quad (9)$$

$$r^2 = 0.910 \qquad C_p = 7.00 \qquad n = 2166$$

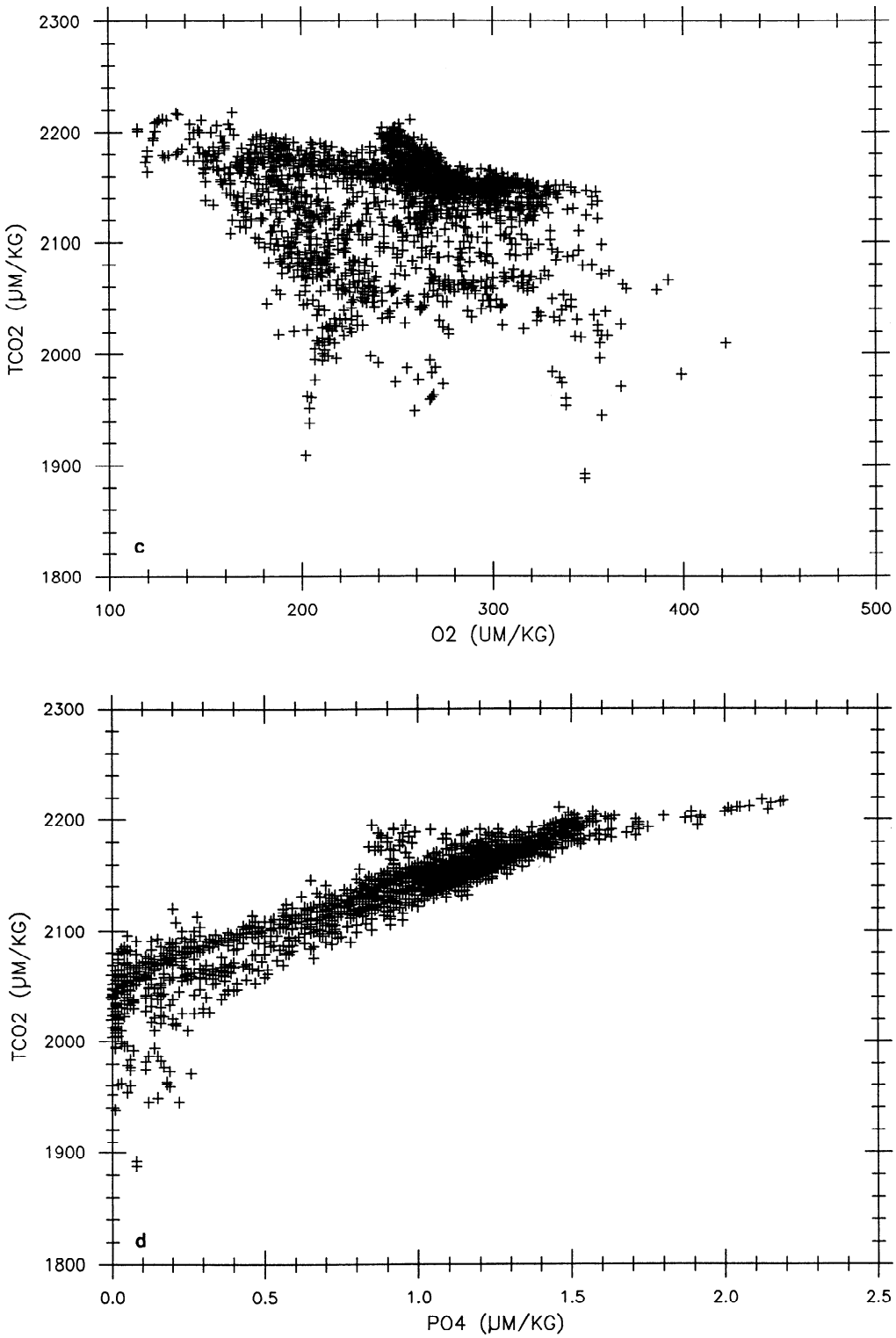

Figure 5. (continued)

It is interesting to note that the coefficient of the NO_3^- term is negative. Geochemically, this makes sense; as the nutrients are consumed, we would expect the alkalinity to increase. The available data set excludes the winter season.

Total CO_2: After determining the correlations between A_T and the hydrographic/nutrient data, we applied a similar multivariate approach to the C_T data. The multiple linear regression in the upper 250 m yielded a "best" regression without including $SiO(OH)_3^-$ (Table 2). While this may seem contrary to function (2), the large difference in exchange rate with the atmosphere between CO_2 and O_2 [*Broecker and Peng*, 1982] helps to make geochemical sense of the decoupling of this relationship (equation (10)) in the upper waters.

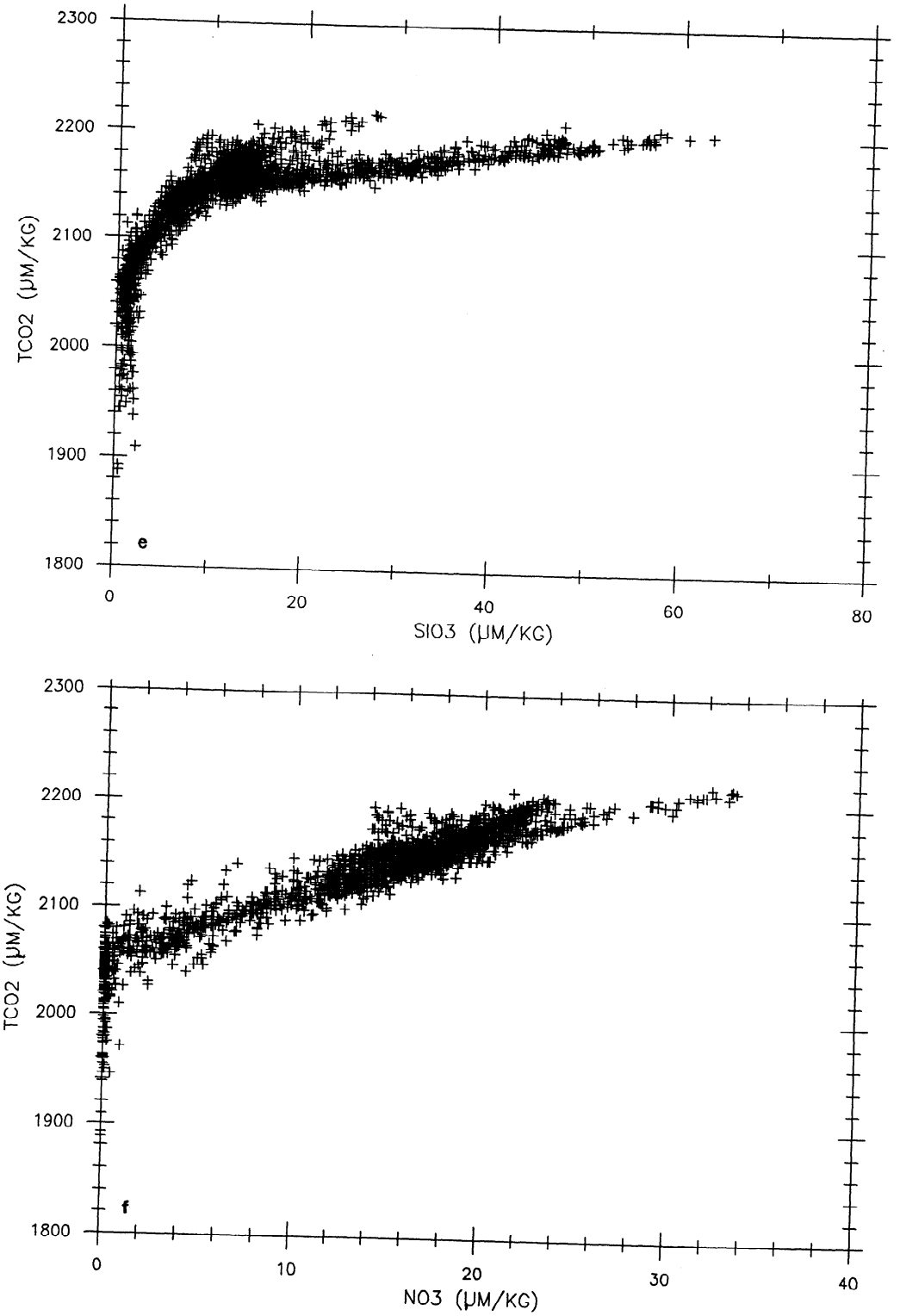

Figure 5. (continued)

Depth ≤ 250 m

$$C_T = 944 + 35.584S - 7.099\theta - 0.464O_2 + 138PO_4^{-3} - 4.62NO_3^- \quad (10)$$

$$r^2 = 0.940 \qquad C_p = 5.14 \qquad n = 623$$

The multiple linear regression of C_T from TTO samples below 250 m yields the relationship

Depth > 250 m

$$C_T = 552 + 44.498S - 4.734\theta - 0.101O_2 + 62.4PO_4^{-3} + 1.20NO_3^- \quad (11)$$

$$r^2 = 0.905 \qquad C_p = 5.98 \qquad n = 2166$$

The lack of a $SiO(OH)_3^-$ term is interesting. Since the dissolution of calcite and aragonite has a large effect on C_T

Table 1. Stepwise Multiple Linear Regression Parameters and Statistics for A_T

Number of Parameters*	r^2	C_p	Intercept	S	θ	O_2	$SiO(OH)_3^-$	PO_4^{-3}	NO_3^-
				Depth ≤ 250 m					
2	0.9690	157.6	599.6	49.017	...	...	...	...	...
3	0.9705	122.8	616.8	48.590	...	...	...	...	−0.348
4	0.9746	21.94	490.2	52.039	...	...	...	56.6	−3.73
5	0.9751	11.14	494.1	51.915	...	...	1.19	53.4	−4.06
6†	0.9754	5.410	530.1	51.132	...	−0.033	0.973	59.3	−4.31
7	0.9754	7.000	528.5	51.032	0.1216	−0.020	0.966	59.8	−4.27
				Depth > 250 m					
2	0.5741	8096	854.3	41.894	...	...	...	...	...
3	0.9021	198.5	333.1	56.227	...	...	1.12	...	...
4	0.9026	188.5	282.7	57.552	...	0.015	1.14	...	...
5	0.9079	62.02	−307.6	73.000	...	0.118	0.985	21.6	...
6	0.9100	14.78	−334.1	73.338	0.9468	0.196	0.981	30.9	...
7‡	0.9104	7.000	−331.6	72.827	0.9480	0.184	0.962	44.6	−0.970

*The number of parameters includes the intercept.
†Equation (8) "best" regression is based on r^2, C_p, and F ratios.
‡Equation (9) "best" regression is based on r^2, C_p, and F ratios.

and is well correlated with $SiO(OH)_3^-$, why then is $SiO(OH)_3^-$ the last term to be entered in the stepwise regression and why is it left out of the "best" regression? The very deep lysocline encountered in the North Atlantic probably provides the explanation [*Biscaye et al.*, 1976].

5.2.2. Implications of regressions. There is no clear relationship between the distributions in Figures 4 and 5 and the sign of all the coefficients. In order to shed more light on the differences between the upper and lower water column regressions, a factor analysis [*Davis*, 1973; *Reyment and Jöreskog*, 1993] on the hydrographic and nutrient data subsets was performed (see Table 3). This analysis was not intended to be a full factor analysis, but rather we seek to identify common groupings (loadings) of our "independent" variables onto axes of lower dimensionality [*Davis*, 1973]. In both the upper and lower water column subsets, only three factors were significant [*Jacobson and Shaw*, 1991]. In the upper water samples, after orthogonal factor rotation [*Davis*, 1973], the nutrients ($SiO(OH)_3^-$, PO_4^{-3}, and NO_3^-) load onto the same factor, θ and O_2 load onto another, and S loads onto the third. In the lower water column PO_4^{-3} and NO_3^- load onto one factor; S, θ, and O_2 load onto another, and $SiO(OH)_3^-$ loads onto the third. Clearly, the nutrients behave similarly in the upper waters and are in some sense redundant, while in the deeper waters $SiO(OH)_3^-$ takes on well-known additional characteristics, driven by the dissolution of opal, not shared by PO_4^{-3} and NO_3^-. The regressions presented here stem from the mathematical "best fit" to the data with few available master variables but are not based on any particular geochemical assumptions.

5.2.3. Implications of residuals. We have computed pH directly from the TTO primary data set in order to produce Figure 1. We can also now provide estimated pH from the results of equations (8) and (10) for the upper layer and equations (9) and (11) for the deep North Atlantic, using purely non-CO_2 system variables. We compare the results in Figure 6. The results show small residuals; once the local correlations are established as above, pH is determined, within ±0.05 units, in the basin simply from other variables. The fact that the correlations are so good in the North Atlantic leads us to believe this technique will work in other ocean basins which typically have less complex hydrography.

Table 2. Stepwise Multiple Linear Regression Parameters and Statistics for C_T

Number of Parameters*	r^2	C_p	Intercept	S	θ	O_2	$SiO(OH)_3^-$	PO_4^{-3}	NO_3^-
				Depth ≤ 250 m					
2	0.7329	2113	2038	...	...	...	...	...	6.99
3	0.8399	1021	1367	18.620	...	...	...	126	...
4	0.9173	230.8	885.7	33.945	−3.8577	...	...	89.7	...
5	0.9320	82.28	1082	32.472	−6.7203	−0.381	...	65.7	...
6†	0.9398	5.141	994.1	35.584	−7.0993	−0.464	...	138.	−4.62
7	0.9398	7.000	995.1	35.564	−7.0960	−0.465	−0.185	139.	−4.58
				Depth > 250 m					
2	0.8213	1910	2067	...	...	...	...	79.2	...
3	0.8434	1409	2361	...	−7.9899	−0.656	...	...	...
4	0.9020	75.89	337.9	49.331	−3.7782	...	...	93.1	...
5	0.9046	16.72	617.7	42.875	−4.7379	−0.124	...	77.7	...
6‡	0.9052	5.982	551.5	44.498	−4.7343	−0.101	...	62.4	1.20
7	0.9052	7.000	521.6	45.280	−4.7299	−0.096	−0.023	65.5	1.09

*The number of parameters includes the intercept.
†Equation (10) "best" regression is based on r^2, C_p, and F ratios.
‡Equation (11) "best" regression is based on r^2, C_p, and F ratios.

Table 3. Factor Structure of the Independent Variables Used in the Regressions

Variable	Factor 1	Factor 2	Factor 3
	Depth ≤ 250 m		
S	−0.14	−0.58	0.80
θ	−0.46	−0.83	0.27
O_2	0.04	0.96	−0.23
$SiO(OH)_3^-$	0.96	0.06	−0.13
PO_4^{-3}	0.94	0.28	−0.15
NO_3^-	0.98	0.14	−0.00
	Depth > 250 m		
S	0.88	−0.43	−0.08
θ	0.93	−0.23	−0.20
O_2	−0.94	−0.33	0.02
$SiO(OH)_3^-$	−0.15	0.41	0.90
PO_4^{-3}	−0.15	0.93	0.32
NO_3^-	−0.03	0.96	0.26

The upper ocean residuals seen in Figures 7a and 7b are about 5% of the true signal size. The range of the A_T measurements in the TTO data set is from 2094 to 2442 μmol kg^{-1}, a total signal amplitude of 348; C_T has an amplitude of 345 μmol kg^{-1} (ranging from 1885 to 2230 μmol kg^{-1}). In the upper 25 m there is substantial scatter (up to ~ ±20%) of this amplitude. Below 250 m, Figure 8 shows a much tighter grouping of data (note scale change), but the majority of these residuals still lie within ±20% because of the reduced range of the measured variables (A_T, 119 μmol kg^{-1}; C_T, 168 μmol kg^{-1}). Nevertheless, in Figure 8 there is clearly some sort of structure to the residuals with depth, particularly for C_T.

The structure seen in the residuals of C_T and A_T implies that not all the information-containing variance has been accounted for in our regressions, particularly equations (9) and (11), and thus future improvements may be expected. The source of this variance is difficult to extract. No doubt the geographic and temporal distribution of the sampling strategy of the TTO program has had an effect here.

An analysis of the residuals displayed in Figure 6 suggests that the accuracy of the regressions of C_T and A_T allows us to calculate pH within the ±0.05 unit necessary to obtain sound absorption coefficients to within ±15%. This useful result may be due, in part, to the compensating errors in the A_T and C_T fields (see Figure 8). The structure in Figure 6 indicates that it may be possible to improve these estimates in the future, perhaps through the use of nonlinear terms. Nevertheless, the clustering of the residuals in Figure 6 indicates an improvement over the NUSC results [*Mellen et al.*, 1987a] by a factor of 6.

5.2.4. Usefulness in other ocean basins. We believe this procedure to be applicable to other ocean basins, in addition to the North Atlantic where we have the best coverage in terms of CO_2 system variables. Similar rules will hold for regions such as the North Pacific. There it may be possible to

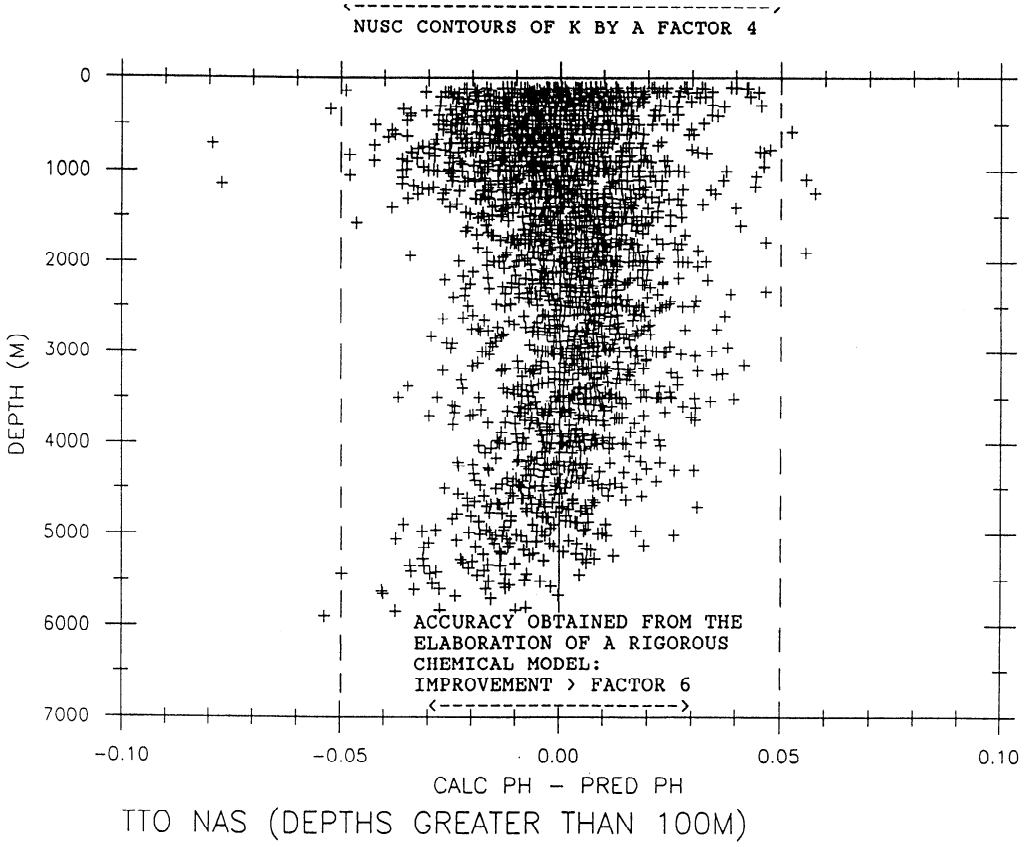

Figure 6. Scatterplot of the pH residuals versus depth. Note that a more stringent improvement factor of 6 (rather than the factor of 4 necessary to produce an accuracy of ±15% in α) still leaves most of the residuals within these bounds.

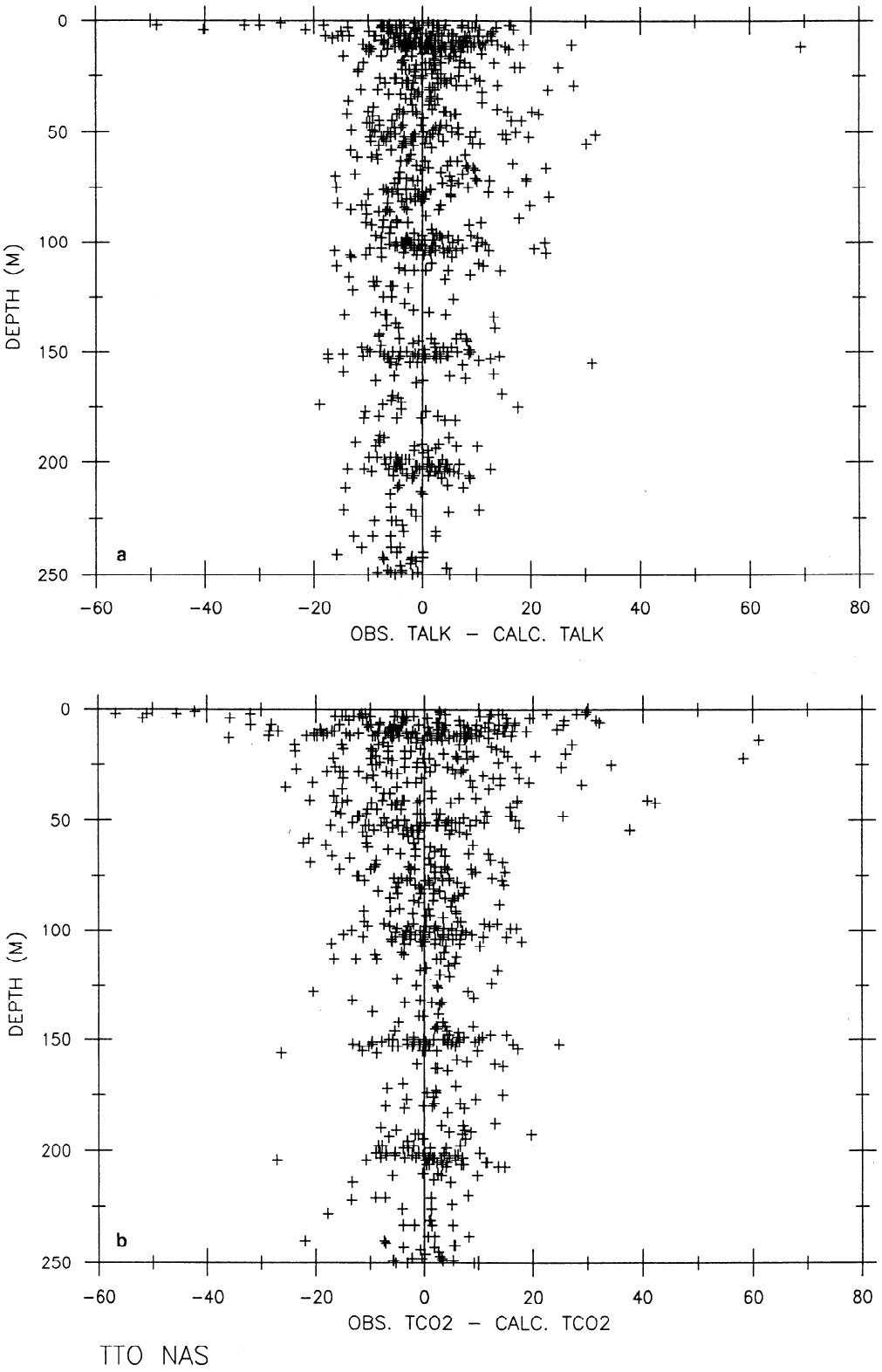

Figure 7. Scatterplot of the residuals versus depth above 250 m: (a) A_T (standard deviation of the residuals, σ_R = 7.8) and (b) C_T (σ_R = 5.9).

make use of the CO_2 system variables measured as part of the GEOSECS program to establish a local correlation between them and the other hydrographic and nutrient data. Once this correlation is established, it will be possible to make use of hydrographic and nutrient data [*Mantyla and Reid*, 1983] to provide a greatly improved estimate of K on a denser geographic grid.

This approach will suffice until global ocean monitoring programs (Joint Global Ocean Flux Study (JGOFS), World Ocean Circulation Experiment (WOCE), etc.) can begin to

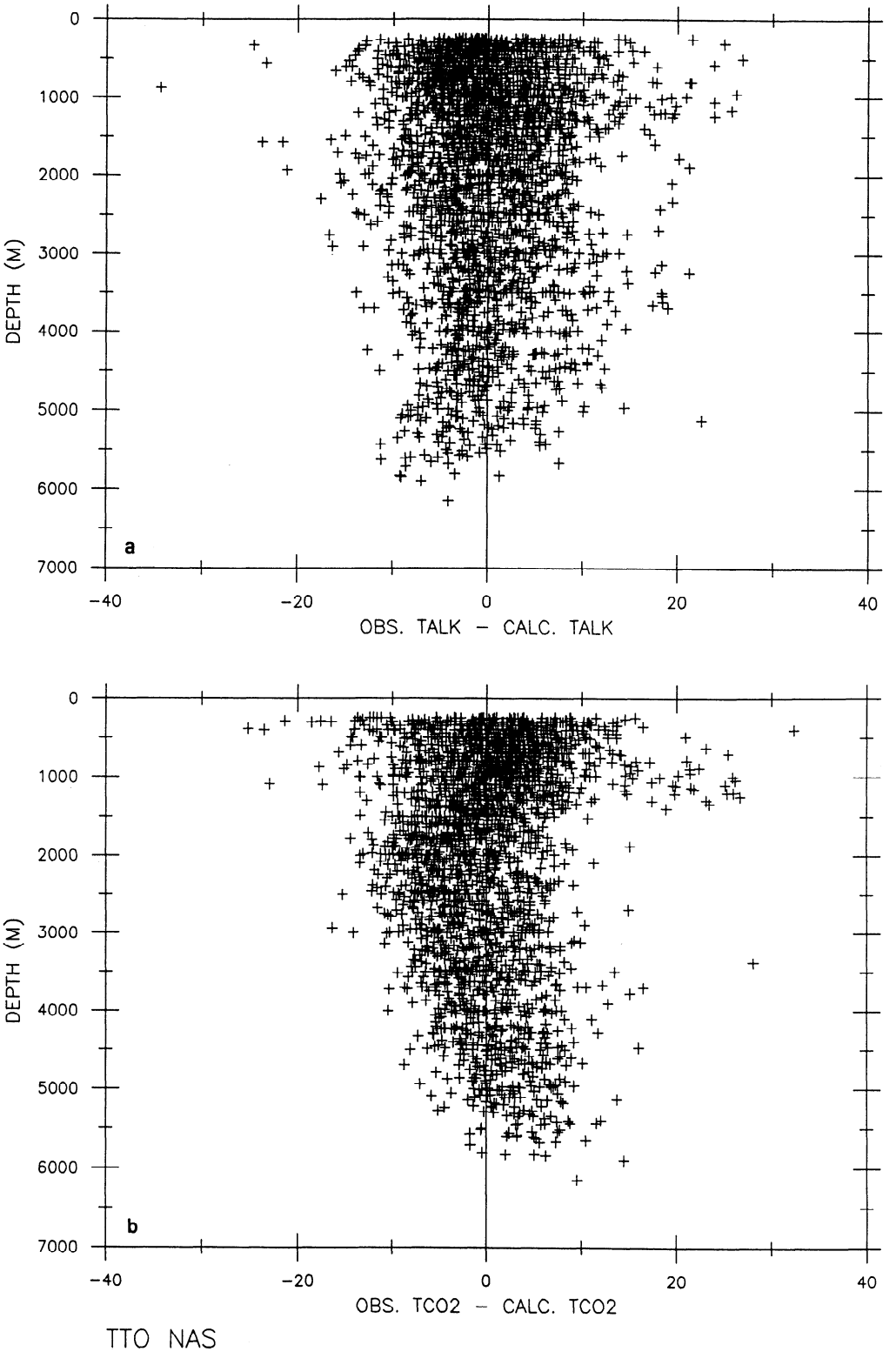

Figure 8. Scatterplot of the residuals versus depth below 250 m: (a) A_T (σ_R = 11.7) and (b) C_T (σ_R = 6.8).

provide CO_2 system variable measurements on a geographic grid more dense than that of GEOSECS. Until these data sets are available, exploration of these correlations can continue to improve our knowledge of the distribution of pH and the sound absorption coefficient in the world oceans. It should also be noted that the other Atlantic data (TTO tropical Atlantic and the South Atlantic Ventilation Experiment) have become or are becoming available.

Studies such as ours provide important insight to sampling strategies needed for global monitoring of the CO_2 system.

For example, interpolation of CO_2 system variables between stations on a densely sampled hydrographic section, or knowledge of the geographic distribution of residuals, can indicate sampling strategies and provide for the most intelligent deployment of expedition resources.

6. Conclusions

After a long history of difficulties in both developing a sound absorption model and measuring CO_2 system variables in seawater, the results presented here for the North Atlantic Ocean suggest that the oceanic pH field can now be defined on a dense geographic grid within the a precision of ± 0.05 pH unit, as required for determining the sound absorption coefficient to within $\pm 15\%$. The extension of this result from the North Atlantic Ocean to other regions is currently under investigation. The results of the present and planned measurements of the carbonate system in the world ocean within the international programs such as JGOFS and WOCE are enlarging the present CO_2 database and will allow us to further refine and extend the validity of these concepts.

In summary, we have evaluated the usefulness of prediction of the ocean pH field from other hydrographic chemical variables. We have further reviewed the various pH scales currently in use by geochemists. We show that the purely non-CO_2 system variables of the TTO North Atlantic data set gives an estimate of the pH field that is superior to the direct estimate provided by the Gorshkov atlas. We suggest our estimates of K be adopted for the North Atlantic. We extend our work by presenting multiple linear regression formulae representing C_T and A_T as linear combinations of more commonly measured hydrographic and nutrient variables in the North Atlantic. Finally, we are ascertaining similar relationships in other ocean basins.

Appendix: Selection of Acidity Constants

The constants as a function of temperature and salinity were selected from the following papers and were corrected, if necessary, to be on the pH of seawater scale: borate, *Dickson* [1990]; phosphate, *Johansson and Wedborg* [1979]; silicate, *Smith and Martell* [1976]; and carbonate, *Goyet and Poisson* [1989].

Acknowledgments. We express our thanks to Anne Edwards for her help in the preparation of the manuscript. We thank Scott Doney for his support and encouragement. The reviews of R. H. Byrne, R. H. Mellen, and an anonymous reviewer were very helpful in strengthening this paper. This work was supported by a grant from the Office of Naval Technology (N00014-90-C-0098). We acknowledge use of the NASA EOS Science Computing Facility at Woods Hole. Woods Hole Oceanographic Institution contribution 8548.

References

Almgren, T., D. Dyrssen, and M. Strandberg, Determination of pH on the moles per kg sea water scale, (M_W), *Deep Sea Res.*, *22*, 635–646, 1975.

Biscaye, P. E., V. Kolla, and K. K. Turekian, Distribution of calcium carbonate in surface sediments of the Atlantic Ocean, *J. Geophys. Res.*, *81*, 2595–2603, 1976.

Bradshaw, A. L., and P. G. Brewer, High precision measurements of alkalinity and total carbon dioxide in seawater by potentiometric titration, 1, Presence of unknown protolyte(s)?, *Mar. Chem.*, *23*, 69–86, 1988a.

Bradshaw, A. L., and P. G. Brewer, High precision measurements of alkalinity and total carbon dioxide in seawater by potentiometric titration, 2, Measurements on standard solutions, *Mar. Chem.*, *24*, 155–162, 1988b.

Bradshaw, A. L., P. G. Brewer, D. K. Shafer, and R. T. Williams, Measurements of total carbon dioxide and alkalinity by potentiometric titration in the GEOSECS program, *Earth Planet. Sci. Lett.*, *55*, 99–115, 1981.

Brewer, P. G., A. L. Bradshaw, and R. T. Williams, Measurements of total carbon dioxide and alkalinity in the North Atlantic Ocean in 1981, in *The Changing Carbon Cycle: A Global Analysis*, edited by T. R. Trabalka and D. E. Reichle, pp. 348–370, Springer-Verlag, New York, 1986.

Broecker, W. S., and T.-H. Peng, *Tracers in the Sea*, 690 pp., Lamont-Doherty Earth Observatory, Palisades, N. Y., 1982.

Byrne, R. H., Standardization of standard buffers by visible spectrometry, *Anal. Chem.*, *59*, 1479–1481, 1987.

Byrne, R. H., and J. A. Breland, High precision multiwavelength pH determinations in seawater using cresol red, *Deep Sea Res.*, *36*, 803–810, 1989.

Davis, J. C., *Statistics and Data Analysis in Geology*, 550 pp., John Wiley, New York, 1973.

Dickson, A. G., Thermodynamics of the dissociation of boric acid in synthetic seawater from 273.15 to 318.15 K, *Deep Sea Res.*, *37*, 755–766, 1990.

Dickson, A. G., The measurement of sea water pH, *Mar. Chem.*, *44*, 131–142, 1993.

Dickson, A. G., and C. Goyet, Handbook of methods for the analysis of the various parameters of the carbon dioxide system in sea water, version 2.0, Program 89-7A, U.S. Dep. of Energy, Washington, D. C., 1993.

Dyrssen, D., and L. G. Sillén, Alkalinity and total carbonate in sea water, A plea for *P-T* independent data, *Tellus*, *19*, 113–121, 1967.

Edmond, J. M., and J. M. T. M. Gieskes, On the calculation of the degree of saturation of sea water with respect to calcium carbonate under in situ conditions, *Geochim. Cosmochim. Acta*, *34*, 1261–1291, 1970.

Efroymson, M. A., Multiple regression analysis, in *Mathematical Methods for Digital Computers*, vol. 1, edited by A. Ralston and H. Wilf, pp. 191–203, John Wiley, New York, 1960.

Eigen, M., and K. Tamm, Sound absorption in electrolytic solutions due to chemical relaxation, *Z. Electrochem.*, *66*, 93–121, 1962.

Goodnight, J. H., A tutorial on the SWEEP operator, *Am. Stat.*, *33*, 149–158, 1979.

Gorshkov, S. G. (Ed.), *World Ocean Atlas*, vol. 2, *Atlantic and Indian Oceans*, Pergamon, New York, 1978.

Goyet, C. M., and P. G. Brewer, Biochemical properties of the oceanic carbon cycle, in *Modeling Oceanic Climate Interactions*, edited by J. Willebrand and D. L. T. Anderson, pp. 271–298, Springer-Verlag, New York, 1993.

Goyet, C. M., and A. Poisson, New determination of carbonic acid dissociation constants in seawater as a function of temperature and salinity, *Deep Sea Res.*, *36*, 1635–1654, 1989.

Jacobson, R. S., and P. R. Shaw, Using the F-test for eigenvalue decomposition problems to find the statistically "optimal" solution, *Geophys. Res. Lett.*, *18*, 1075–1078, 1991.

Jin Guoliang and P. F. Worcester, The feasibility of measuring ocean pH by long-range acoustics, *J. Geophys. Res.*, *94*, 4749–4756, 1989.

Johansson, O., and M. Wedborg, Stability constants of phosphoric acid in seawater of 5–40‰ salinity and temperatures 5–25°C, *Mar. Chem.*, *8*, 57–69, 1979.

Keeling, C. D., Carbon dioxide in surface ocean waters, 4, Global distribution, *J. Geophys. Res.*, *73*, 4543–4553, 1968.

Khoo, K. H., R. W. Ramette, C. H. Bulberson, and R. G. Bates, Determination of hydrogen ion concentrations in seawater from 5 to 40°C: Standard potentials at salinities from 20 to 45‰, *Anal. Chem.*, *49*, 29–34, 1977.

Leonard, R. W., P. C. Combs, and L. R. Skidmore, Attenuation of sound in synthetic sea water, *J. Acoust. Soc. Am.*, *21*, 63, 1949.

Mallows, C. L., Some comments on C_p, *Technometrics*, *15*, 661–675, 1973.

Mantyla, A., and J. Reid, Abyssal characteristics of the world oceans, *Deep Sea Res.*, *30*, 805–833, 1983.

Mellen, R. H., P. M. Scheifele, and D. G. Browning, Global model for sound absorption in sea water, Scientific and engineering

studies, *Tech. Rep. 7923*, Nav. Underwater Syst. Cent., Newport, R.I., 1987a.

Mellen, R. H., P. M. Scheifele, and D. G. Browning, Global model for sound absorption in sea water, 2, GEOSECS *p*H data analysis, *Tech. Rep. 7925*, Sci. and Eng. Stud., Nav. Underwater Syst. Cent., 1987b.

Millero, F. J., The thermodynamics of the carbonate system in seawater, *Geochim. Cosmochim. Acta, 43*, 1651–1661, 1979.

Millero, F. J., The *p*H of estuarine waters, *Limnol. Oceanogr., 31*, 839–847, 1986.

Peng, T.-H., T. Takahashi, W. S. Broecker, and J. Olafsson, Seasonal variability of carbon dioxide, nutrients and oxygen in the northern North Atlantic surface water: Observations and a model, *Tellus, 39*, 439–458, 1987.

Qiu Xinfang, Effect of ocean environmental factors on sound absorption by boric acid relaxation in sea water, *Acta Oceanol. Sin., 10*(2), 271–280, 1991.

Redfield, A. C., The processes determining the concentration of oxygen, phosphate and other organic derivatives within the depths of the Atlantic Ocean, *Pap. Phys. Oceanogr. Meteorol., 9*(2), 1–22, 1942.

Reyment, R. A., and K. G. Jöreskog, *Applied Factor Analysis in the Natural Sciences*, 371 pp., Cambridge University Press, New York, 1993.

Schulkin, M., and H. W. Marsh, Sound absorption in sea water, *J. Acoust. Soc. Am., 42*, 864–865, 1962.

Smith, R. M., and A. E. Martell, *Critical Stability Constants*, vol. 4, 257 pp., Plenum, New York, 1989.

Stumm, W., and J. J. Morgan, *Aquatic Chemistry*, 2nd ed., 780 pp., John Wiley, New York, 1981.

Thorp, W. H., Deep ocean sound attenuation in the sub and low kilocycle-per-second region, *J. Acoust. Soc. Am., 38*, 648–654, 1965.

UNESCO, Thermodynamics of carbon dioxide system in seawater, Report by the carbon dioxide subpanel of the JPOTS, *UNESCO Tech. Pap. Mar. Sci., 51*, 55 pp., 1987.

P. G. Brewer, Monterey Bay Aquarium Research Institute, Pacific Grove, CA 93950.

D. M. Glover (corresponding author), C. Goyet, and D. K. Shafer, Department of Marine Chemistry and Geochemistry, Woods Hole Oceanographic Institution, Woods Hole, MA 02543. (e-mail: dglover@whoi.edu)

(Received December 15, 1993; revised November 10, 1994; accepted November 30, 1994.)